ACS OMEGA

Article

Cite This: ACS Omega 2018, 3, 6642−6650

Enzymatic Synthesis of Glycerol Carbonate Using a Lipase Immobilized on Magnetic Organosilica Nanoflowers as a Catalyst

Yingjie Du,[†] Jing Gao,*[,†,‡] Weixi Kong,[†] Liya Zhou,[†] Li Ma,[†] Ying He,[†] Zhihong Huang,[†] and Yanjun Jiang*[,†,‡]

[†]School of Chemical Engineering and Technology and [‡]National-Local Joint Engineering Laboratory for Energy Conservation of Chemical Process Integration and Resources Utilization, Hebei University of Technology, No. 8 Guangrong Road, Hongqiao District, Tianjin 300130, China

Supporting Information

ABSTRACT: For synthesizing glycerol carbonate (GC) by a reaction between glycerol (GL) and dimethyl carbonate (DMC), a lipase immobilized on magnetic organosilica nanoflowers was prepared and utilized as a biocatalyst. *Candida antarctica* lipase B (CALB) was chosen as a model enzyme for preparing an immobilized biocatalyst (CALB@nanoflowers). The obtained CALB@nanoflowers was characterized using scanning electron microscopy, transmission electron microscopy, and confocal laser scanning microscopy. Effects of GL/DMC molar ratio, biocatalyst amount, temperature, surfactant and molecular sieve addition, and reaction time on the conversion of GL and the selectivity of CALB@nanoflowers were investigated. The optimal catalytic performance (yield of GC: 88.66% and conversion of GL: 94.24%) was achieved under the condition of 1:20 molar ratio of GL to DMC with 0.2 g of molecular sieves added at 50 °C for 24 h. After recycling seven times, the CALB@nanoflowers maintained over 79% of its initial activity and the yield of GC was 70.31%.

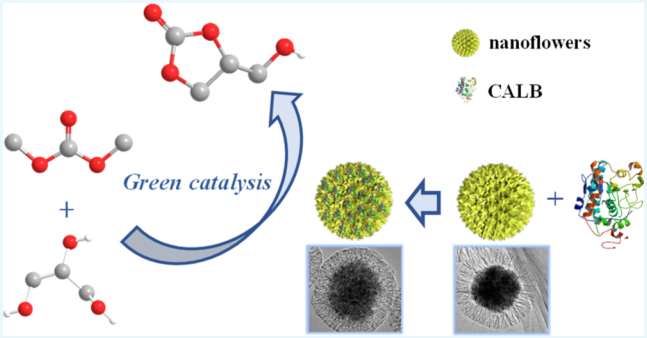

1. INTRODUCTION

With the biodiesel manufacture fast developed, a large amount of glycerol (GL) was obtained.[1,2] GL can be used in various industries such as textiles, foods, drugs, and cosmetics, and it can also be a platform molecule in high-value chemical synthesis after purification.[3] Recently, researchers have transformed GL into a multitude of high value-added chemicals such as ethers, propanediols, bulk chemicals, and glycerol carbonate (GC).[3−6]

GC (4-hydroxymethyl-1,3-dioxolan-2-one) is one of the most important value-added products that can be derived from GL.[5,7,8] Because of its ideal physicochemical properties including low toxicity, high boiling point, nonflammability, and good biodegradability, GC has been adopted as a green solvent for chemical maquillages, skincare products, and medicine.[9] GC was also used as an additive of chemical coatings, paints, and detergents as well as a precursor of polycarbonates and polyurethanes.[10,11] Studies for developing procedures of GC synthesis have drawn much attention these years because of its potential industrial applications in various sectors.[12]

In previous reports, chemical catalysts were usually adopted for transesterification of GL with dimethyl carbonate (DMC) to produce GC.[7,13,14] However, the drawbacks including high energy requirements, low catalyst recovery rate, and high pollution of the environment are major disadvantages in chemical catalyzed synthesis processes.[12,15−17] Enzymatic transesterification of GL with DMC was considered to be one of the compelling candidates of chemical catalysis as a green catalysis route.[18,19] According to the literature, the reactions include transesterification, hydrolysis, and the further intramolecular cyclization process, and then equimolar GL and DMC are required by the reaction stoichiometry.[20] However, the side reaction is influenced by various factors such as the reagent ratio of GL/DMC, the type of catalysts, and temperature.[21] Thus, various factors should be considered and investigated in the process of GC synthesis.

Lipases (triacylglycerol ester hydrolase, EC 3.1.1.3), a kind of green catalyst, are widely used in hydrolysis, esterification, cyclo-esterification, and transesterification reactions in consideration of their outstanding chemo-, region-, and stereoscopic-selective performances.[22,23] As we all know, lipases perform catalysis via a peculiar catalytic mechanism known as interfacial activation. Interfacial activation is the phenomenon that an oligopeptide blocks the active center of lipases under the normal environment and exposes the activity center under hydrophobic interface.[24−28] However, free lipase was usually limited by easily deactivation, poor use stability particularly

Received: April 18, 2018
Accepted: June 7, 2018
Published: June 20, 2018

DOI: 10.1021/acsomega.8b00746
ACS Omega 2018, 3, 6642−6650

that difficulties to be reusable.[29] Fortunately, lipases immobilized onto solid carriers could overcome these weaknesses effectively.[30−32] Immobilization techniques can maintain the activity of enzymes and improve their stability. If materials and methods can be properly designed, immobilization can also improve many enzyme features, for example, selectivity, specificity, thermal stability, and reusability.[33−36]

Up to now, various solid supports (e.g., silica, polymer, carbon, and some composite materials) have been demonstrated to be able to immobilize lipases.[23,37,38] It is worth mentioning that the activity and stability of the immobilized catalysts can be increase a lot in nonaqueous solvents while the carriers with hydrophobic surfaces due to the hydrophobic-cap structure and interfacial effect of the lipase.[39−41] Recently, a novel kind of organosilica nanoflower with a magnetic Fe_3O_4 core and a flowerlike organosilica radial-wrinkle shell was reported by our group.[40] The remarkable properties of novel magnetic organosilica nanoflowers make them perfect supports for lipase immobilization: (1) The flowerlike organosilica with a radial-wrinkle shell around the magnetic Fe_3O_4 core can reduce the inevitable aggregation of magnetic nanoparticles.[42−44] (2) The hydrophobicity of organosilica can promote the catalytic performance of lipases.[45,46] (3) A large specific surface area of the nanoflowers can enhance the enzyme loading and promote the mass transfer. It has to be explained that a favorable temperature and gentle stirring are important to gain a uniform flowerlike organosilica radial-wrinkle shell.[40] Additionally, magnetic core−shell nanoparticles have been adopted as supports for enzyme immobilization because of the ease of separation by magnetic fields.[42,43] When lipases are immobilized on magnetic nanoparticles, the composites can be easily separated from the reaction medium, which can improve the reusability of the enzyme.[44]

Thus, in this work, magnetic organosilica nanoflowers have been chosen as a carrier for immobilizing *Candida antarctica* lipase B (CALB) via covalent binding method to construct nanobiocatalysts named CALB@nanoflowers.[40,47] CALB, a typical lipase, has been commonly used as an industrial enzyme. The amphiphilic α-helix in CALB, also called a lid, can shelter the active site from the substrate or be removed in the hydrophobic environment for exposing the active center to substrate.[48] Then, CALB@nanoflowers was used as a catalyst for the transesterification of GL with DMC and the follow-up cyclo-esterification in the synthesis of GC for the first time (Scheme 1).

Scheme 1. Preparation of CALB@Nanoflowers and Synthesis of GC Catalyzed by CALB@Nanoflowers

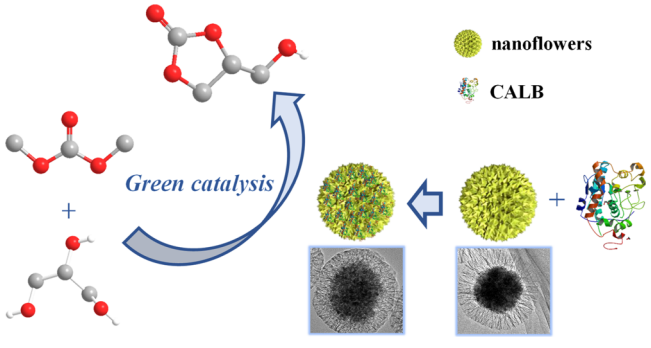

In particular, the transesterification of GL with DMC is a kinetically controlled reaction, which means that the enzyme properties and activation of substrate may influence transient maximum yields.[34,35,49,50] The magnetic CALB@nanoflowers was characterized by scanning electron microscopy (SEM), transmission electron microscopy (TEM) and confocal laser scanning microscopy (CLSM). Factors that would affect the yield of GC and the selectivity of CALB@nanoflowers were investigated in detail. Meanwhile, the catalytic activity of this catalyst was compared with those of the reported biocatalysts. Reusability of the magnetic CALB@nanoflowers was also appraised.

2. RESULTS AND DISCUSSION

2.1. Characterization of Nanoflowers and CALB@Nanoflowers. As shown in the SEM image (Figure 1a), the

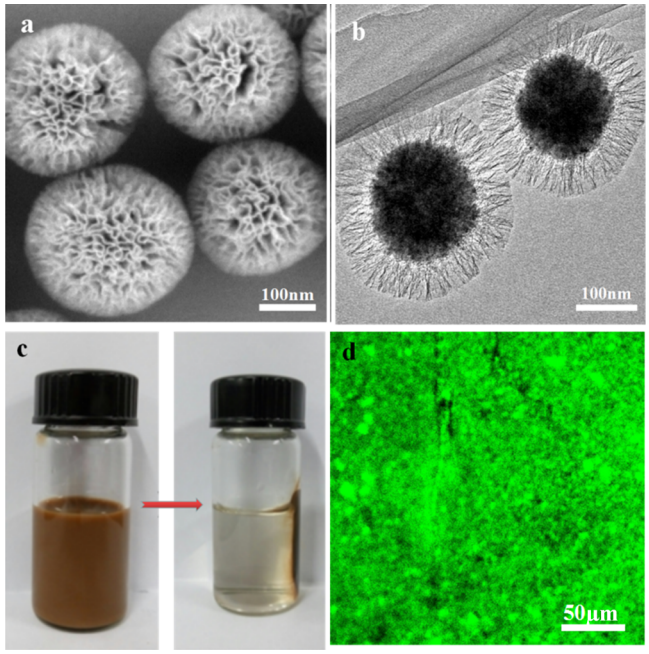

Figure 1. (a) SEM image of the silica nanoflowers; (b) TEM image of the silica nanoflowers; (c) photographs of CALB@nanoflowers separated from aqueous solution by a magnet; and (d) CLSM image of the FITC-labeled CALB@nanoflowers.

nanoflowers are particles that have a well-proportioned size of ∼270 nm and an obvious flowerlike morphology. As shown in Figure S1, the width of radial-wrinkle perpendicular channels is about 14 nm, which was consistent with the result of our previous report.[40] The TEM image showed that the nanoflowers had a core−shell structure and the thickness of the organosilica shell was ca. 45 nm (Figure 1b). The results recorded on a vibrating sample magnetometer verified the satisfactory magnetism of nanoflowers (62 emu/g) and CALB@nanoflowers (37 emu/g).

Similar to other magnetic nanoparticles, the nanoparticles can be separated easily by a magnet (Figure 1c) rather than a centrifuge, which may reduce the costs of industrial application.[51] To verify the success of immobilization, fluorescein isothiocyanate-labeled CALB (FITC-CALB) was immobilized by nanoflowers. As shown in Figure 1d, the fluorescence of the immobilized enzyme particles proved the successful immobilization of CALB on nanoflowers.[52,53] Under

DOI: 10.1021/acsomega.8b00746
ACS Omega 2018, 3, 6642−6650

the optimal immobilization conditions, the maximum loading of CALB on the nanoflowers was 93 mg/$g_{support}$ while the specific enzyme activity was 244.1 U/$mg_{protein}$.[40] Compared with the specific enzyme activity of free CALB (647.6 U/$mg_{protein}$), the activity recovery is 37.69%.

2.2. Synthesis of GC. The production of GC was performed based on the transesterification reaction between GL (1) and DMC (2) using CALB@nanoflowers as a catalyst. According to the literature,[20,21] the reaction mechanism is presented in Figure 2. Interactions between GL and DMC lead

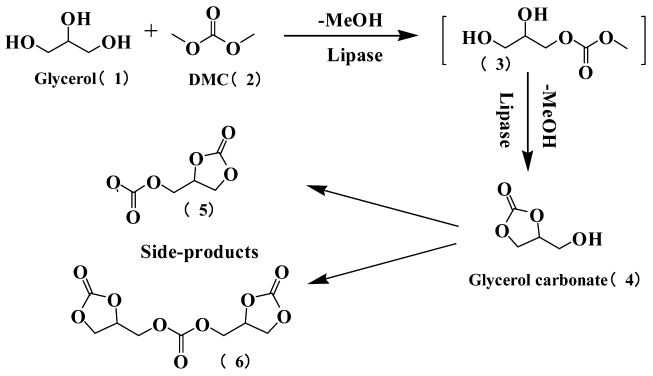

Figure 2. Scheme of GC synthesis from GL with DMC catalyzed by a lipase.

to a short-life intermediate (3) and methanol. Further, intramolecular cyclization of the short-life intermediate causes it to remove one molecular methanol and generate GC (4). Side products of this reaction might be glycerol dicarbonate (GDC) (5) or diglycerol tricarbonate (DGTC) (6).[16]

The reaction was investigated in detail in the presence of CALB@nanoflowers under various reaction conditions for improving GL conversion and catalyst selectivity and reducing side reaction. Otherwise, several solvents were adopted to investigate the effect of solvents on the conversion of GL and the selectivity of immobilized enzyme.[16] As shown in Figure S2, the added organic solvents are adverse to the reaction. Thus, a solvent-free system was adopted in the subsequent research.[21]

2.3. Effect of GL/DMC Molar Ratio. The influence of the molar ratio of GL to DMC on GL conversion and catalyst selectivity is depicted in Figure 3. As shown in Figure 2, the reaction stoichiometry requires a molar ratio of GL to DMC of

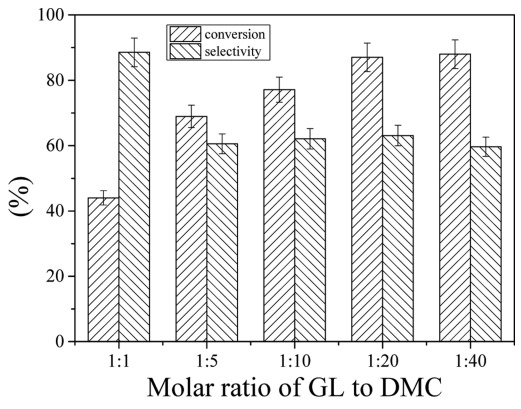

Figure 3. GL conversion and the CALB@nanoflowers selectivity with different GL/DMC molar ratios.

1:1 and 1 mol of GL can yield 1 mol of GC in theory.[54] As presented in Figure 3, the transformation of GL increased from 44.01 to 87.03% with changing the GL/DMC ratio from 1:1 to 1:20. With further increase of DMC, the transformation of GL increases negligibly. GC was synthesized at a low GL/DMC ratio; subsequently, the side product formed with increasing DMC amounts and the selectivity of the CALB@nanoflowers decreased by raising the GL/DMC ratios from 1:1 to 1:20.

The reason might be that GL owns two types of hydroxyl and the two primary alcohol groups are more active than the secondary hydroxyl group, and it also leads to higher selectivity.[55,56] Otherwise, the turbidity of the reaction mixture increased with the increase of DMC concentration, which reduces the interaction of CALB@nanoflowers with GL, thereby reducing conversion.[54] Especially, the conversion and selectivity seem to change little while the GL/DMC ratio changes from 1:20 to 1:40. Therefore, in the subsequent experiments, 1:20 ratio of GL to DMC was chosen for attaining not only high transformation of GL but also acceptable selectivity.

2.4. Effect of Biocatalyst Concentration. The biocatalyst concentration also exerts a significant effect on the conversion of GL. As shown in Figure 4, conversion of GL was

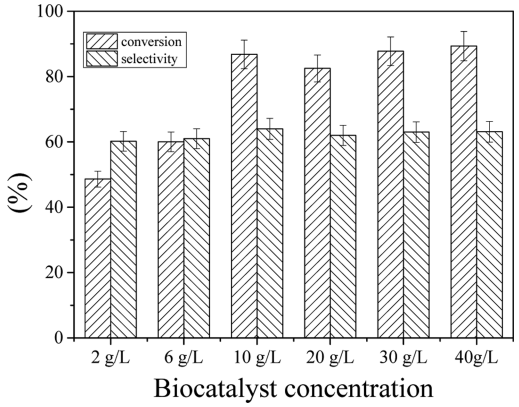

Figure 4. GL conversion and the CALB@nanoflowers selectivity with different biocatalyst concentrations.

increased from 48.63 to 86.78% as the CALB@nanoflowers concentration was increased from 2 to 10 g/L in a solvent-free system. The GL conversion was not significantly increased from 86.78 to 89.32% with further increasing the CALB@nanoflowers concentration from 10 to 40 g/L, whereas the selectivity suffers a slight decrease in this range of biocatalyst concentrations (2−40 g/L).

The yield of GC decreased because the amount of enzyme is excess for achieving a maximum yield. Once the maximum yield has been achieved under a 10 g/L catalyst concentration at 24 h, excess catalyst only can be used to make side product during the transesterification reaction.[57,58] Under this condition, part of the GC is converted to GDC or DGTC by the excess catalysts, and then the GC yield did not increase, though the conversion and selectivity changed slightly.[59] A concentration of 10 g/L was chosen for achieving economy application and sufficiently high performances in subsequent experiments.

2.5. Effect of Molecular Sieve Addition. To select proper molecular sieve addition for GC production, different amounts of molecular sieves (0, 0.2, 0.4, 0.8, and 1.6 g) were

DOI: 10.1021/acsomega.8b00746
ACS Omega 2018, 3, 6642−6650

used in this experiment. As illustrated by the results in Figure 5, the conversion of GL was increased from 71.96 to 86.78%

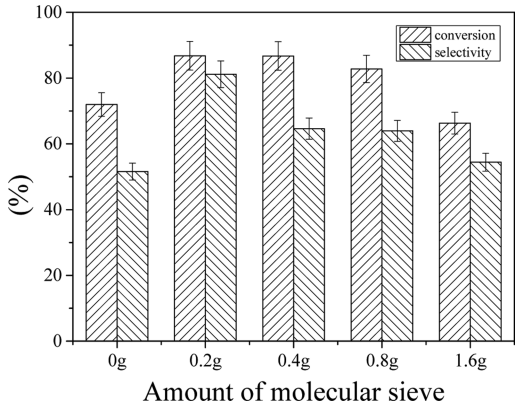

Figure 5. GL conversion and CALB@nanoflowers selectivity with different amounts of molecular sieve addition.

with 0.2 g of molecular sieves being added. Further increasing the amount of molecular sieves added to 1.6 g, GL conversion was decreased to 66.28%. The same phenomenon was observed for the selectivity of the biocatalyst. As one of the products, inevitably produced methanol has an inhibitory effect on enzyme activity and stability. Although a certain amount of water is required for acquisition and maintenance of lipase activity, excess water also triggers many enzyme inactivation processes.[60,61] Molecular sieves can remove excess water in the solvent-free system. However, excess molecular sieves can reduce the reaction rate by adsorbing the essential water, which can restrain the interactions between enzyme and substrate.[19] Thus, 0.2 g of molecular sieves was enough to maintain essential water content in a microenvironment and was selected in the further tests.

2.6. Effect of Temperature. Temperature plays a significant role in affecting the viscosity of the reaction mixture, activation energy of substrate, and the activity of enzyme.[12] Thus, the reaction temperature was investigated.

As shown in Figure 6, conversion of GL increased from 46.25 to 94.24% with the temperature being increased from 40 to 50 °C. With the temperature being further increased to 70 °C, the conversion of GL decreased to 68.98% and the selectivity of CALB@nanoflowers was decreased from 97.81 to 74.60%. A high reaction temperature might lead to the loss of

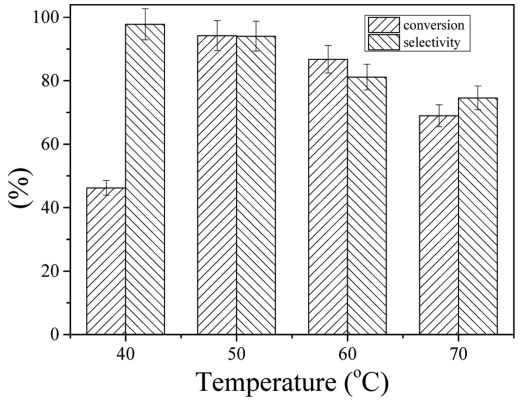

Figure 6. GL conversion and CALB@nanoflowers selectivity at different temperatures.

enzyme activity and selectivity because of the thermal denaturation.[16] Deactivation of the enzyme makes it difficult to maintain a high GL conversion and also may reduce the yield of GC. Therefore, 50 °C was chosen as an optimal temperature.

2.7. Effect of Reaction Time. The effect of reaction time was researched in detail with the range of 1−27 h, and the results are shown in Figure 7. It can be found that a GL

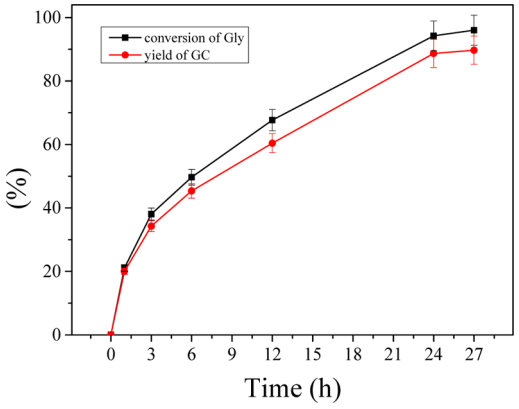

Figure 7. GL conversion and CALB@nanoflowers selectivity with different reaction times.

conversion of 38.05% and a GC yield of 34.27% were obtained at 3 h. The increase of reaction time to 6 h gave 67.67% conversion of GL and 60.40% yield of GC. As the kinetically controlled synthesis reaction,[49,50] under the optimal conditions from above experiments, the reaction almost established kinetic equilibrium after 24 h (94.24% of GL conversion and 88.66% of GC yield). Further lengthening of reaction time to 27 h had a slight influence on both the conversion and the yield. Thus, 24 h was used in the subsequent reactions.

2.8. Effect of Surfactant Addition. In the traditional process of GC production, the hydrophilic GL and the hydrophobic DMC are nonmiscible. A surfactant that contains both hydrophilic and hydrophobic components might solve the problem efficiently by reducing the surface tension at the interface between the substrates and helping reactants to mix well.[62,63] Thus, to further increase the GC yield, Tween 20, Tween 80, and Triton X-100 (10%, v/v) were added during the reaction process.

As shown in Figure 8, the addition of Triton X-100 enhanced the GL conversion from 94.24 to 96.25% and the selectivity of CALB@nanoflowers was also increased, which was similar to previous report.[63] In contrast, the conversion of GL and the selectivity of CALB@nanoflowers were decreased by adding Tween 20 (68.93 and 82.86%) and Tween 80 (76.63 and 85.71%) in comparison with the control experiments (94.24 and 94.08%). This phenomenon might be due to the fact that the system viscosity was increased, which caused the mass transfer resistance to increase, while surfactants were added.[62]

2.9. Reusability of CALB@Nanoflower. The reusability of the CALB@nanoflowers was researched at optimized condition for GC production. For comparison, CALB immobilized on core−shell magnetic pure silica spheres with a flowerlike morphology (named CALB@MMPS) and Novozym 435 (N435) with the same initial activity were also tested in the same condition. The results are depicted in

DOI: 10.1021/acsomega.8b00746
ACS Omega 2018, 3, 6642−6650

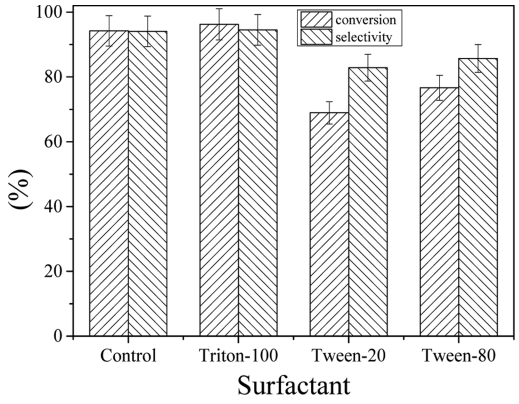

Figure 8. GL conversion and CALB@nanoflowers selectivity with different surfactants.

Figure 9. After recycling seven times, the CALB@nanoflowers maintained more than 79% of its initial activity and the yield of

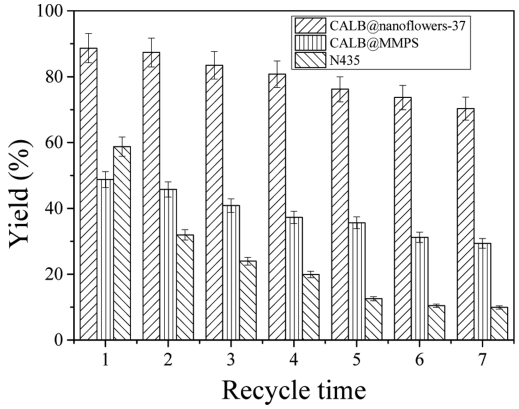

Figure 9. Reusability of CALB@nanoflowers and other immobilized lipases in GC production.

GC was 70.31%, which were much higher than those of CALB@MMPS (ca. 60 and 29.37%) and commercial N435 (ca. 17 and 9.898%). The CALB@nanoflowers maintained about 84% of its initial selectivity (94.13%), whereas the CALB@MMPS and commercial N435 maintained about 80 and 65% of their initial selectivity, respectively (90.25 and 93.15%).

The better reusability of the CALB@nanoflowers than N435 in this reaction can be due to the fact that immobilization of CALB on mesoporous materials could prevent interprotein polymerization more availably than the immobilization of CALB on macroporous materials.[40] The performance of CALB@nanoflowers is obviously superior to that of CALB@MMPS, which can be interpreted by the following reasons. First of all, covalent immobilization is a better method to link enzyme molecules to solid carriers, providing little leakage than the adsorption method.[64,65] Second, it can also be attributed to the hydrophobicity of the nanoflowers.[40,45] Hydrophobic nanoflowers have more appetency to attract hydrophobic substrates than hydrophilic MMPS, which obviously increased the apparent activity of the CALB@nanoflowers in non-aqueous phase reaction.[39,41,46]

2.10. Biological Conversion of GL to GC Using Various Biocatalysts. The comparison of the catalytic activity of CALB@nanoflowers with those of other reported biocatalysts in the conversion of GL into GC is provided in Table 1. It was found that N435 exhibited excellent activity during the transesterification in a cosolvent system, but the product was difficult to be separated from the substrate−solvent−product mixture.[55,62,67] For a solvent-free system, various catalysts have been investigated for the GC synthesis, including N435, cross-linked enzyme aggregate onto magnetic particles (CLEMPA), *Aspergillus niger* (AN), and lipase-linked magnetic macro-/nanoparticles (lipase-MP_3).[16,21,68−70] Compared with reported biocatalysts, CALB@nanoflowers had high catalytic activity and even retained a high catalytic efficiency with a GC yield of 70.31% after recycling seven times (Figure 9). The relatively high GC yield and high recyclability demonstrated that CALB@nanoflowers was an efficient biocatalyst for the transesterification of GL with DMC. These results thereby suggested that CALB@nanoflowers had great potential in industrial applications.

3. CONCLUSIONS

This work was contributed to optimize the condition of enzymatic production of GC from glycerolation of DMC catalyzed by an innovative immobilized lipase (CALB@nanoflowers) in an eco-friendly route. At the optimum conditions of the amount of enzyme (5 g/L), molecular sieves (0.2 g), and GL/DMC molar ratio (1:20), the yield of GC was 88.66% at 50 °C after 24 h in the solvent-free system. In general, these results implied that CALB@nanoflowers can efficiently be used as a catalyst to develop an enzymatic route for GC synthesis.

4. MATERIALS AND METHODS

4.1. Materials and Reagents. Cetyltrimethylammonium bromide (CTAB) was purchased from Sigma-Aldrich. CALB and N435 were bought from Novozymes (China) Biotechnol-

Table 1. Comparison of the Performance of Different Biocatalysts Used in GL Transesterification[66,a]

catalyst type	molar ratio (GL/DMC)	temperature (°C)	reaction time (h)	catalyst loading	solvent	*Y*, *C*, or *S* (%)	references
CALB@nanoflowers	1:20	50	24	5 g/L	−	Y = 88.53, S = 94.13	this work
N435	1:2	60	48	75 g/L	acetonitrile	Y = 96	62
N435	1:1	60	30	54 wt %	THF	Y = 88, S = 93	55
N435	1:1.5	60	14	22.02 wt %	*t*-butanol	C = 94.85	67
N435	1:10	70	48	5 wt %	−	Y = 80, S = 86	68
CLEMPA	1:10	60	6	28.6 wt %	−	Y = 55, S = 90	69
AN	1:10	60	4	12 wt %	−	Y = 59.3, S = 80.3	16
lipase-MP_3	1:10	60	6	2−8 wt %	−	Y = 41.31, S = 85	70
CLEMPA	1:10	60	6	5 wt %	−	Y = 32.4, S = 90	21

[a] Y = GC yield; C = GL conversion; S = Y/C (selectivity); "−" = solvent-free system.

DOI: 10.1021/acsomega.8b00746
ACS Omega 2018, 3, 6642−6650

ogy Co. Ltd. 1,2-Bis(trimethylsilyl)ethane (BTSE), GL, and DMC were purchased from Shandong Xiya Industrial Co., Ltd. Tetraethoxysilane (TEOS), hexahydrate ferric chloride ($FeCl_3 \cdot 6H_2O$), anhydrous sodium acetate, cyclohexanol, *tert*-butanol, anhydrous ethanol, ethanediol, acetonitrile, hexamethylene and diaminomethanal of analytical purity were purchased from Tianjin Chemical Co., Ltd. Glutaraldehyde, acetone, *n*-hexane, and (3-aminopropyl)triethoxysilane (APTES) were purchased from Tianjin Alfa Aesar Chemical Co., Ltd. All agents were used without further purification.

4.2. Preparation of the Magnetic Organosilica Nanoflowers and CALB@Nanoflowers. *4.2.1. Synthesis of Magnetic Organosilica Nanoflowers.* Briefly, an aqueous solution of diaminomethanal (0.4 M, 100 g) was added into a round-bottom flask with 0.3 g of the as-prepared Fe_3O_4 particles. Then, a solution containing CTAB (1.25 g), *n*-butyl alcohol (1.25 g), cyclohexane (5 g), and a mixture of TEOS (0.875 g) and BTSE (0.375 g) were added orderly at 25 °C under gentle stirring for 30 min. When the temperature was raised to 70 °C, the reaction continues for another 24 h under gentle stirring. To remove the templates, the nanoflowers were dispersed in 250 mL of acetone, refluxed at 80 °C for 48 h, and dried at 60 °C for 12 h.[40]

4.2.2. Synthesis of CALB@Nanoflowers. Before the immobilization of lipase, the nanoflowers were amino-functionalized by APTES and were activated by glutaraldehyde (0.4 wt %).[40] The activated nanoflowers (glutaraldehyde nanoflowers, 100 mg) were dispersed in 5 mL of phosphate buffer solution (PBS, 0.1 M, pH 7.0) by ultrasonication for 10 min. Then, 5 mL of CALB solution (4.128 mg/mL) was added, and the mixed solution was shaken (170 rpm) for 1 h. The products were washed with PBS (0.1 M, pH 7.0) three times.

4.3. Synthesis of GC. The reaction was carried out using a 48 mL seal pressure tubing under water bath condition. Typically, 5 mmol of GL and 50 mmol of DMC were added into the reactor, followed by the addition of CALB@nanoflowers (30 g/L). The mixture was incubated by a thermostatic shaker (170 rpm) at 60 °C and kept for 24 h. Then, it was cooled to room temperature, and CALB@nanoflowers was separated by a magnet.

For exact analysis, 0.1 g of *tert*-butanol was added as an internal standard to determine the GC and GL. After diluting by 10 mL of *tert*-butanol, the product mixture was analyzed by a gas chromatograph form Shimadzu (GC-2010 Plus) with a flame ionization detector and a KB-1 capillary column (50 m × 0.32 mm × 0.25 μm) using nitrogen as the carrier gas (2.28 mL/min). Injector and detector temperatures were 300 and 280 °C, respectively. The oven temperature started at 100 °C, which was held for 3 min, followed by upping to 150 °C at a 10 °C·min^{-1} rising rate and ramping of 15 °C·min^{-1} up to 200 °C, and lasted for 12.33 min. All computational formulas are detailed in the Supporting Information.

4.4. Optimization of Reaction Conditions. *4.4.1. Effect of the Molar Ratio of GL to DMC.* The effect of molar ratio of GL/DMC on the conversion of GL and the selectivity of immobilized enzyme was investigated at various GL/DMC molar ratios (1:1, 1:5, 1:10, 1:20, and 1:40). In a solvent-free system, the mixture of GL (2.5 mmol), DMC (different amount), CALB@nanoflowers (30 g/L), and molecular sieves (0.8 g) was shaken in a thermostatic shaker at 60 °C for 24 h.

4.4.2. Effect of Catalyst Concentration. The effect of catalyst concentration on the conversion of GL and the selectivity of immobilized enzyme was investigated at various enzyme concentrations (2, 6, 10, 20, 30, and 40 g/L). In a solvent-free system, the mixture of GL (2.5 mmol), DMC (50 mmol), CALB@nanoflowers, molecular sieves (0.8 g) was shaken in a thermostatic shaker at 60 °C for 24 h.

4.4.3. Effect of Molecular Sieve Concentration. The effect of amount of molecular sieves on the conversion of GL and the selectivity of immobilized enzyme was investigated at various amounts of molecular sieves (0, 0.2, 0.4, 0.8, and 1.6 g). In a solvent-free system, the mixture of GL (2.5 mmol), DMC (50 mmol), CALB@nanoflowers (10 g/L), different mounts of molecular sieves was shaken in a thermostatic shaker at 60 °C for 24 h.

4.4.4. Effect of Temperature. To investigate the effect of temperature on the conversion of GL and the selectivity of immobilized enzyme, the reactions were performed at different temperatures (40, 50, 60, and 70 °C). In a solvent-free system, the mixture of GL (2.5 mmol), DMC (50 mmol), CALB@nanoflowers (10 g/L), molecular sieves (0.2 g) was shaken in a thermostatic shaker at 60 °C for 24 h at different temperatures.

4.4.5. Effect of Surfactant Addition. To investigate the effect of surfactant on the conversion of GL and the selectivity of immobilized enzyme, several kinds of surfactants (Tween 20, Triton X-100, and Tween 80, 10 v/v %) were added. In a solvent-free system, the mixture of GL (2.5 mmol), DMC (50 mmol), CALB@nanoflowers (10 g/L), molecular sieves (0.2 g), and surfactant (10 v/v %) was shaken in a thermostatic shaker at 60 °C for 24 h.

4.4.6. Effect of Reaction Time. In a solvent-free system, the mixture of GL (2.5 mmol), DMC (50 mmol), CALB@nanoflowers (10 g/L), molecular sieves (0.2 g), and Triton X-100 (10%, v/v) was shaken in a thermostatic shaker at 50 °C. The progress was computed by measuring the amount of GL and GC during the reaction.

4.5. Reusability of CALB@Nanoflower. Reusabilities of the CALB@nanoflowers and N435 were compared by repetitive uses in the transesterification of GL with DMC at optimal conditions. CALB@nanoflowers and N435 were magnetically and centrifugally recovered from reaction media, respectively, followed by the washing with DMC several times before being used in the next reaction batch.

■ ASSOCIATED CONTENT

Supporting Information

The Supporting Information is available free of charge on the ACS Publications website at DOI: 10.1021/acsomega.8b00746.

Experimental details, estimations, nitrogen adsorption−desorption isotherms and pore size distribution profile, and effect of various organic solvents on the transformation rate of glycerol and the selectivity of immobilized enzyme (PDF)

■ AUTHOR INFORMATION

Corresponding Authors

*E-mail: yanjunjiang@hebut.edu.cn. Phone: 86-22-60204945. Fax: 86-22-60204294 (Y.J.).

*E-mail: jgao@hebut.edu.cn. Phone: 86-22-60202416 (J.G.).

ORCID

Yanjun Jiang: 0000-0003-1470-2102

Notes

The authors declare no competing financial interest.

DOI: 10.1021/acsomega.8b00746
ACS Omega 2018, 3, 6642−6650

■ ACKNOWLEDGMENTS

This work was supported by the National Nature Science Foundation of China (nos. 21576068, 21276060, 21276062, and 21306039), the Natural Science Foundation of Tianjin (16JCYBJC19 800), the Natural Science Foundation of Hebei Province (B2015202082, B2016202027, and B2017202056), the Program for Top 100 Innovative Talents in Colleges and Universities of Hebei Province (SLRC2017029), Hebei high level personnel of support program (A2016002027), and the Graduate Innovation Support Program in Hebei Province (CXZZSS2017024).

■ ABBREVIATIONS

GC, glycerol carbonate; GL, glycerol; DMC, dimethyl carbonate; GDC, glycerol dicarbonate; DGTC, diglycerol tricarbonate; CALB, *Candida antarctica* lipase B; CTAB, cetyltrimethylammonium bromide; N435, Novozym 435; BTSE, 1,2-bis(trimethylsilyl)ethane; TEOS, tetraethyl orthosilicate; APTES, (3-aminopropyl)triethoxysilane; CALB@nanoflowers, lipase immobilized on magnetic organosilica nanoflower

■ REFERENCES

(1) Leão, R. A. C.; de Souza, S. P.; Nogueira, D. O.; Silva, G. M. A.; Silva, M. V. M.; Gutarra, M. L. E.; Miranda, L. S. M.; Castro, A. M.; Junior, I. I.; de Souza, R. O. M. A. Consecutive lipase immobilization and glycerol carbonate production under continuous-flow conditions. *Catal. Sci. Technol.* **2016**, *6*, 4743−4748.

(2) Yang, F.; Hanna, M. A.; Sun, R. Value-added uses for crude glycerol–a byproduct of biodiesel production. *Biotechnol. Biofuels* **2012**, *5*, 13.

(3) Zhou, C.-H.; Beltramini, J. N.; Fan, Y.-X.; Lu, G. Q. Chemoselective catalytic conversion of glycerol as a biorenewable source to valuable commodity chemicals. *Chem. Soc. Rev.* **2008**, *37*, 527−549.

(4) Pazhavelikkakath Purushothaman, R. K.; van Haveren, J.; van Es, D. S.; Melián-Cabrera, I.; Heeres, H. J. The oxidative esterification of glycerol to methyl glycerate in methanol using gold on oxidic supports: an insight in product selectivity. *Green Chem.* **2012**, *14*, 2031−2037.

(5) Wang, Y.; Zhou, J.; Guo, X. Catalytic hydrogenolysis of glycerol to propanediols: a review. *RSC Adv.* **2015**, *5*, 74611−74628.

(6) Zhu, S.; Zhu, Y.; Hao, S.; Zheng, H.; Mo, T.; Li, Y. One-step hydrogenolysis of glycerol to biopropanols over Pt-H4SiW12O40/ZrO2 catalysts. *Green Chem.* **2012**, *14*, 2607−2616.

(7) Luo, X.; Ge, X.; Cui, S.; Li, Y. Value-added processing of crude glycerol into chemicals and polymers. *Bioresour. Technol.* **2016**, *215*, 144−154.

(8) Sun, D.; Yamada, Y.; Sato, S.; Ueda, W. Glycerol as a potential renewable raw material for acrylic acid production. *Green Chem.* **2017**, *19*, 3186−3213.

(9) Gu, Y.; Jérôme, F. Bio-based solvents: an emerging generation of fluids for the design of eco-efficient processes in catalysis and organic chemistry. *Chem. Soc. Rev.* **2013**, *42*, 9550−9570.

(10) Le Roux, E. Recent advances on tailor-made titanium catalysts for biopolymer synthesis. *Coord. Chem. Rev.* **2016**, *306*, 65−85.

(11) Liu, S.; Wang, X. Polymers from carbon dioxide: Polycarbonates, polyurethanes. *Curr. Opin. Green Sustain. Chem.* **2017**, *3*, 61−66.

(12) Wang, S.; Hao, P.; Li, S.; Zhang, A.; Guan, Y.; Zhang, L. Synthesis of glycerol carbonate from glycerol and dimethyl carbonate catalyzed by calcined silicates. *Appl. Catal., A* **2017**, *542*, 174−181.

(13) Lee, J.; Jung, J.-M.; Oh, J.-I.; Sik Ok, Y.; Kwon, E. E. Establishing a green platform for biodiesel synthesis via strategic utilization of biochar and dimethyl carbonate. *Bioresour. Technol.* **2017**, *241*, 1178−1181.

(14) Ochoa-Gómez, J. R.; Gómez-Jiménez-Aberasturi, O.; Ramírez-López, C.; Maestro-Madurga, B. Synthesis of glycerol 1,2-carbonate by transesterification of glycerol with dimethyl carbonate using triethylamine as a facile separable homogeneous catalyst. *Green Chem.* **2012**, *14*, 3368−3376.

(15) Ishak, Z. I.; Sairi, N. A.; Alias, Y.; Aroua, M. K. T.; Yusoff, R. Production of glycerol carbonate from glycerol with aid of ionic liquid as catalyst. *Chem. Eng. J.* **2016**, *297*, 128−138.

(16) Tudorache, M.; Protesescu, L.; Coman, S.; Parvulescu, V. I. Efficient bio-conversion of glycerol to glycerol carbonate catalyzed by lipase extracted from Aspergillus niger. *Green Chem.* **2012**, *14*, 478−482.

(17) Wang, X.; Zhang, P.; Cui, P.; Cheng, W.; Zhang, S. Glycerol carbonate synthesis from glycerol and dimethyl carbonate using guanidine ionic liquids. *Chin. J. Chem. Eng.* **2017**, *25*, 1182−1186.

(18) Franssen, M. C. R.; Steunenberg, P.; Scott, E. L.; Zuilhof, H.; Sanders, J. P. M. Immobilised enzymes in biorenewables production. *Chem. Soc. Rev.* **2013**, *42*, 6491−6533.

(19) Jo, Y. J.; Lee, O. K.; Lee, E. Y. Dimethyl carbonate-mediated lipid extraction and lipase-catalyzed in situ transesterification for simultaneous preparation of fatty acid methyl esters and glycerol carbonate from Chlorella sp. KR-1 biomass. *Bioresour. Technol.* **2014**, *158*, 105−110.

(20) Rokicki, G.; Rakoczy, P.; Parzuchowski, P.; Sobiecki, M. Hyperbranched aliphatic polyethers obtained from environmentally benign monomer: glycerol carbonate. *Green Chem.* **2005**, *7*, 529−539.

(21) Tudorache, M.; Negoi, A.; Protesescu, L.; Parvulescu, V. I. Biocatalytic alternative for bio-glycerol conversion with alkyl carbonates via a lipase-linked magnetic nano-particles assisted process. *Appl. Catal., B* **2014**, *145*, 120−125.

(22) dos Santos, J. C. S.; Rueda, N.; Sanchez, A.; Villalonga, R.; Gonçalves, L. R. B.; Fernandez-Lafuente, R. Versatility of divinylsulfone supports permits the tuning of CALB properties during its immobilization. *RSC Adv.* **2015**, *5*, 35801−35810.

(23) Fernandez-Lafuente, R. Lipase from Thermomyces lanuginosus: Uses and prospects as an industrial biocatalyst. *J. Mol. Catal. B: Enzym.* **2010**, *62*, 197−212.

(24) Derewenda, Z. S. Structure and Function of Lipases. *Adv. Protein Chem.* **1994**, *45*, 1−52.

(25) Verger, R. 'Interfacial activation' of lipases: facts and artifacts. *Trends Biotechnol.* **1997**, *15*, 32−38.

(26) Mancheño, J. M.; Pernas, M. A.; Martínez, M. J.; Ochoa, B.; Rúa, M. L.; Hermoso, J. A. Structural Insights into the Lipase/esterase Behavior in the Candida rugosa Lipases Family: Crystal Structure of the Lipase 2 Isoenzyme at 1.97Å Resolution. *J. Mol. Biol.* **2003**, *332*, 1059−1069.

(27) Stergiou, P.-Y.; Foukis, A.; Filippou, M.; Koukouritaki, M.; Parapouli, M.; Theodorou, L. G.; Hatziloukas, E.; Afendra, A.; Pandey, A.; Papamichael, E. M. Advances in lipase-catalyzed esterification reactions. *Biotechnol. Adv.* **2013**, *31*, 1846−1859.

(28) Greco-Duarte, J.; Cavalcanti-Oliveira, E. D.; Da Silva, J. A. C.; Fernandez-Lafuente, R.; Freire, D. M. G. Two-step enzymatic production of environmentally friendly biolubricants using castor oil: Enzyme selection and product characterization. *Fuel* **2017**, *202*, 196−205.

(29) Hernandez, K.; Fernandez-Lafuente, R. Lipase B from Candida antarctica immobilized on octadecyl Sepabeads: A very stable biocatalyst in the presence of hydrogen peroxide. *Process Biochem.* **2011**, *46*, 873−878.

(30) Cipolatti, E. P.; Manoel, E. A.; Fernandez-Lafuente, R.; Freire, D. M. G. Support engineering: relation between development of new supports for immobilization of lipases and their applications. *Biotechnol. Res. Innovat.* **2017**, *1*, 26−34.

(31) Cui, J.; Zhao, Y.; Feng, Y.; Lin, T.; Zhong, C.; Tan, Z.; Jia, S. Encapsulation of Spherical Cross-Linked Phenylalanine Ammonia Lyase Aggregates in Mesoporous Biosilica. *J. Agric. Food Chem.* **2017**, *65*, 618−625.

(32) Zhao, Z.; Tian, J.; Wu, Z.; Liu, J.; Zhao, D.; Shen, W.; He, L. Enhancing enzymatic stability of bioactive papers by implanting

DOI: 10.1021/acsomega.8b00746
ACS Omega 2018, 3, 6642−6650

enzyme-immobilized mesoporous silica nanorods into paper. *J. Mater. Chem. B* **2013**, *1*, 4719−4722.
(33) Manoel, E. A.; dos Santos, J. C. S.; Freire, D. M. G.; Rueda, N.; Fernandez-Lafuente, R. Immobilization of lipases on hydrophobic supports involves the open form of the enzyme. *Enzyme Microb. Technol.* **2015**, *71*, 53−57.
(34) Garcia-Galan, C.; Berenguer-Murcia, Á.; Fernandez-Lafuente, R.; Rodrigues, R. C. Potential of different enzyme immobilization strategies to improve enzyme performance. *Adv. Synth. Catal.* **2011**, *353*, 2885−2904.
(35) Rodrigues, R. C.; Ortiz, C.; Berenguer-Murcia, Á.; Torres, R.; Fernández-Lafuente, R. Modifying enzyme activity and selectivity by immobilization. *Chem. Soc. Rev.* **2013**, *42*, 6290−6307.
(36) Du, Y.; Gao, J.; Zhou, L.; Ma, L.; He, Y.; Huang, Z.; Jiang, Y. Enzyme nanocapsules armored by metal-organic frameworks: A novel approach for preparing nanobiocatalyst. *Chem. Eng. J.* **2017**, *327*, 1192−1197.
(37) Chen, Z.; Zhao, C.; Ju, E.; Ji, H.; Ren, J.; Binks, B. P.; Qu, X. Design of Surface-Active Artificial Enzyme Particles to Stabilize Pickering Emulsions for High-Performance Biphasic Biocatalysis. *Adv. Mater.* **2016**, *28*, 1682−1688.
(38) Lin, Y.; Li, Z.; Chen, Z.; Ren, J.; Qu, X. Mesoporous silica-encapsulated gold nanoparticles as artificial enzymes for self-activated cascade catalysis. *Biomaterials* **2013**, *34*, 2600−2610.
(39) Chen, Y.; Shi, J. Chemistry of Mesoporous Organosilica in Nanotechnology: Molecularly Organic-Inorganic Hybridization into Frameworks. *Adv. Mater.* **2016**, *28*, 3235−3272.
(40) Gao, J.; Kong, W.; Zhou, L.; He, Y.; Ma, L.; Wang, Y.; Yin, L.; Jiang, Y. Monodisperse core-shell magnetic organosilica nanoflowers with radial wrinkle for lipase immobilization. *Chem. Eng. J.* **2017**, *309*, 70−79.
(41) Gascón, V.; Díaz, I.; Blanco, R. M.; Márquez-Álvarez, C. Hybrid periodic mesoporous organosilica designed to improve the properties of immobilized enzymes. *RSC Adv.* **2014**, *4*, 34356−34368.
(42) Hou, C.; Wang, Y.; Ding, Q.; Jiang, L.; Li, M.; Zhu, W.; Pan, D.; Zhu, H.; Liu, M. Facile synthesis of enzyme-embedded magnetic metal-organic frameworks as a reusable mimic multi-enzyme system: mimetic peroxidase properties and colorimetric sensor. *Nanoscale* **2015**, *7*, 18770−18779.
(43) Patel, S. K. S.; Choi, S. H.; Kang, Y. C.; Lee, J.-K. Eco-Friendly Composite of Fe3O4-Reduced Graphene Oxide Particles for Efficient Enzyme Immobilization. *ACS Appl. Mater. Interfaces* **2017**, *9*, 2213−2222.
(44) Pashangeh, K.; Akhond, M.; Karbalaei-Heidari, H. R.; Absalan, G. Biochemical characterization and stability assessment of Rhizopus oryzae lipase covalently immobilized on amino-functionalized magnetic nanoparticles. *Int. J. Biol. Macromol.* **2017**, *105*, 300−307.
(45) Zhou, Z.; Inayat, A.; Schwieger, W.; Hartmann, M. Improved activity and stability of lipase immobilized in cage-like large pore mesoporous organosilicas. *Microporous Mesoporous Mater.* **2012**, *154*, 133−141.
(46) Zhou, Z.; Piepenbreier, F.; Marthala, V. R. R.; Karbacher, K.; Hartmann, M. Immobilization of lipase in cage-type mesoporous organosilicas via covalent bonding and crosslinking. *Catal. Today* **2015**, *243*, 173−183.
(47) Barbosa, O.; Torres, R.; Ortiz, C.; Fernandez-Lafuente, R. Versatility of glutaraldehyde to immobilize lipases: Effect of the immobilization protocol on the properties of lipase B from Candida antarctica. *Process Biochem.* **2012**, *47*, 1220−1227.
(48) Zisis, T.; Freddolino, P. L.; Turunen, P.; van Teeseling, M. C. F.; Rowan, A. E.; Blank, K. G. Interfacial Activation of Candida antarctica Lipase B: Combined Evidence from Experiment and Simulation. *Biochemistry* **2015**, *54*, 5969−5979.
(49) Kasche, V. Mechanism and yields in enzyme catalysed equilibrium and kinetically controlled synthesis of β-lactam antibiotics, peptides and other condensation products. *Enzyme Microb. Technol.* **1986**, *8*, 4−16.
(50) Kasche, V.; Galunsky, B. Ionic strength and pH effects in the kinetically controlled synthesis of benzylpenicillin by nucleophilic deacylation of pree and immobilized phenyl-acetyl-penicillin amidase with 6-aminopenicillanic acid. *Biochem. Biophys. Res. Commun.* **1982**, *104*, 1215−1222.
(51) Kalantari, M.; Kazemeini, M.; Tabandeh, F.; Arpanaei, A. Lipase immobilisation on magnetic silica nanocomposite particles: effects of the silica structure on properties of the immobilised enzyme. *J. Mater. Chem.* **2012**, *22*, 8385−8393.
(52) Bolivar, J. M.; Eisl, I.; Nidetzky, B. Advanced characterization of immobilized enzymes as heterogeneous biocatalysts. *Catal. Today* **2016**, *259*, 66−80.
(53) Secundo, F. Conformational changes of enzymes upon immobilisation. *Chem. Soc. Rev.* **2013**, *42*, 6250−6261.
(54) Simanjuntak, F. S. H.; Kim, T. K.; Lee, S. D.; Ahn, B. S.; Kim, H. S.; Lee, H. CaO-catalyzed synthesis of glycerol carbonate from glycerol and dimethyl carbonate: Isolation and characterization of an active Ca species. *Appl. Catal., A* **2011**, *401*, 220−225.
(55) Kim, S. C.; Kim, Y. H.; Lee, H.; Yoon, D. Y.; Song, B. K. Lipase-catalyzed synthesis of glycerol carbonate from renewable glycerol and dimethyl carbonate through transesterification. *J. Mol. Catal. B: Enzym.* **2007**, *49*, 75−78.
(56) Stewart, J. A.; Drexel, R.; Arstad, B.; Reubsaet, E.; Weckhuysen, B. M.; Bruijnincx, P. C. A. Homogeneous and heterogenised masked N-heterocyclic carbenes for bio-based cyclic carbonate synthesis. *Green Chem.* **2016**, *18*, 1605−1618.
(57) Algoufi, Y. T.; Kabir, G.; Hameed, B. H. Synthesis of glycerol carbonate from biodiesel by-product glycerol over calcined dolomite. *J. Taiwan Inst. Chem. Eng.* **2017**, *70*, 179−187.
(58) Lu, J.; Nie, K.; Xie, F.; Wang, F.; Tan, T. Enzymatic synthesis of fatty acid methyl esters from lard with immobilized Candida sp. 99-125. *Process Biochem.* **2007**, *42*, 1367−1370.
(59) Sonnati, M. O.; Amigoni, S.; Taffin de Givenchy, E. P.; Darmanin, T.; Choulet, O.; Guittard, F. Glycerol carbonate as a versatile building block for tomorrow: synthesis, reactivity, properties and applications. *Green Chem.* **2013**, *15*, 283−306.
(60) Volkin, D. B.; Staubli, A.; Langer, R.; Klibanov, A. M. Enzyme thermoinactivation in anhydrous organic solvents. *Biotechnol. Bioeng.* **1991**, *37*, 843−853.
(61) Fiorani, G.; Perosa, A.; Selva, M. Dimethyl carbonate: a versatile reagent for a sustainable valorization of renewables. *Green Chem.* **2018**, *20*, 288−322.
(62) Jung, H.; Lee, Y.; Kim, D.; Han, S. O.; Kim, S. W.; Lee, J.; Kim, Y. H.; Park, C. Enzymatic production of glycerol carbonate from by-product after biodiesel manufacturing process. *Enzyme Microb. Technol.* **2012**, *51*, 143−147.
(63) Tudorache, M.; Negoi, A.; Parvulescu, V. I. Enhancement of the valorization of renewable glycerol: The effects of the surfactant-enzyme interaction on the biocatalytic synthesis of glycerol carbonate. *Catal. Today* **2017**, *279*, 71−76.
(64) Barbosa, O.; Ortiz, C.; Berenguer-Murcia, Á.; Torres, R.; Rodrigues, R. C.; Fernandez-Lafuente, R. Glutaraldehyde in bio-catalysts design: a useful crosslinker and a versatile tool in enzyme immobilization. *RSC Adv.* **2014**, *4*, 1583−1600.
(65) Virgen-Ortíz, J. J.; Tacias-Pascacio, V. G.; Hirata, D. B.; Torrestiana-Sanchez, B.; Rosales-Quintero, A.; Fernandez-Lafuente, R. Relevance of substrates and products on the desorption of lipases physically adsorbed on hydrophobic supports. *Enzyme Microb. Technol.* **2017**, *96*, 30−35.
(66) Teng, W. K.; Ngoh, G. C.; Yusoff, R.; Aroua, M. K. A review on the performance of glycerol carbonate production via catalytic transesterification: Effects of influencing parameters. *Energy Convers. Manage.* **2014**, *88*, 484−497.
(67) Lanjekar, K.; Rathod, V. K. Utilization of glycerol for the production of glycerol carbonate through greener route. *J. Environ. Chem. Eng.* **2013**, *1*, 1231−1236.
(68) Lee, K. H.; Park, C.-H.; Lee, E. Y. Biosynthesis of glycerol carbonate from glycerol by lipase in dimethyl carbonate as the solvent. *Bioprocess Biosyst. Eng.* **2010**, *33*, 1059−1065.
(69) Tudorache, M.; Nae, A.; Coman, S.; Parvulescu, V. I. Strategy of cross-linked enzyme aggregates onto magnetic particles adapted to

DOI: 10.1021/acsomega.8b00746
ACS Omega 2018, 3, 6642−6650

the green design of biocatalytic synthesis of glycerol carbonate. *RSC Adv.* **2013**, *3*, 4052−4058.
(70) Tudorache, M.; Protesescu, L.; Negoi, A.; Parvulescu, V. I. Recyclable biocatalytic composites of lipase-linked magnetic macro-/nano-particles for glycerol carbonate synthesis. *Appl. Catal., A* **2012**, *437*−*438*, 90−95.

DOI: 10.1021/acsomega.8b00746
ACS Omega 2018, 3, 6642−6650